

Thermal exchange bias field drifts after 10 keV He ion bombardment: Storage temperature dependence and initial number of coupling sites

Christoph Schmidt, Tanja Weis, Dieter Engel, and Arno Ehresmann

Citation: [Journal of Applied Physics](#) **110**, 113911 (2011); doi: 10.1063/1.3665198

View online: <http://dx.doi.org/10.1063/1.3665198>

View Table of Contents: <http://scitation.aip.org/content/aip/journal/jap/110/11?ver=pdfcov>

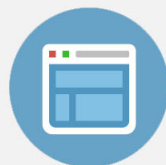
Published by the [AIP Publishing](#)

Advertisement:



Re-register for Table of Content Alerts

Create a profile.



Sign up today!



Thermal exchange bias field drifts after 10 keV He ion bombardment: Storage temperature dependence and initial number of coupling sites

Christoph Schmidt,^{a)} Tanja Weis, Dieter Engel, and Arno Ehresmann
*Institute of Physics and Center for Interdisciplinary Nanostructure Science and Technology (CINSaT),
 University of Kassel, Heinrich-Plett-Str. 40, 34132 Kassel, Germany*

(Received 25 August 2011; accepted 28 October 2011; published online 8 December 2011)

Sputter deposited Mn₈₃Ir₁₇(30 nm)/Co₇₀Fe₃₀(10 nm)/Ta thin films have been investigated for their thermal exchange bias field drift at different storage temperatures after 10 keV He⁺ ion bombardment in an externally applied in-plane magnetic field. It is experimentally shown that the drift coefficient in an intermediate time interval, as given in a recently developed model, is proportional to T and proportional to the initial number of coupling sites in the polycrystalline exchange bias layer system used. © 2011 American Institute of Physics. [doi:10.1063/1.3665198]

I. INTRODUCTION

Exchange biased ferromagnet/antiferromagnet bilayers are used for magnetic reference electrodes in hard disk read heads¹ or other magnetoresistive sensor elements.² Therefore, the thermal stability of the magnetic characteristics (exchange bias (EB) field, H_{EB} , and coercive field, H_C) is of the highest importance for such industrial applications. Without an additional annealing step, however, the exchange bias field changes temporally after layer deposition in a magnetic field.³ In the past few years, it has been shown that this temporal change of H_{EB} is intimately connected with the local anisotropy constant^{4,5} and grain size distribution⁶ of the involved polycrystalline layer systems. The possibility of tailoring H_{EB} in direction⁷ and magnitude⁸ in many EB layer systems⁹ by keV-He ion bombardment (IB) has been demonstrated some time ago. These ion bombardment modified exchange bias systems have been shown to work in magnetoresistive sensors^{2,10} and logic elements¹¹ as well as for the fabrication of artificial magnetic domains.^{12–15} Therefore, for EB layer systems modified by ion bombardment it is also important to understand whether and why there is a thermal drift of H_{EB} after ion bombardment.

In a first systematic study, the temporal drift of H_{EB} after 10 keV He ion bombardment has been investigated at room temperature.¹⁶ Therefore, a tentative model has been developed to describe the observed almost logarithmic increase of H_{EB} with time. One of the predictions of the developed model¹⁶ is a characteristic storage temperature dependence of the logarithmic change rate of H_{EB} (with or without ion bombardment). In the current study we present the results of investigations on the temporal changes of the EB field for different temperatures after ion bombardment and an analysis of the published data without ion bombardment.

II. EXPERIMENT

The preparation, characterization, and modification of the thin film system Mn₈₃Ir₁₇(30 nm)/Co₇₀Fe₃₀(10 nm)/Ta(3 nm) with a buffer layer of 50 nm Cu has been previ-

ously described.¹⁶ Briefly, the EB fields of the used samples after field cooling ($H_{EB,0}$) at 528 K for 60 min in a field of 40 kA/m are between 8.2 and 9.3 kA/m. A magneto-optical Kerr effect magnetometer in longitudinal geometry has been used to characterize the sample's magnetization reversal and for the determination of the exchange bias field. The ion bombardment was performed at room temperature by using 10 keV He⁺ ions with a fluence of 1.0×10^{15} ions/cm² at a base pressure of 1.0×10^{-6} mbar. The in-plane magnetic field, $\vec{H}_{IB} = 80$ kA/m, during IB was oriented *parallel* or *antiparallel* to the field direction during field cooling¹⁷ (in the following, briefly designated as *parallel* or *antiparallel* bombardment field geometry).

For the experimental determination of the temporal change of the exchange bias field, hysteresis loops have been recorded in intervals of 60 min, with the first loop 1 h after ion bombardment. After one day, the intervals were increased gradually from 4 h to 3 days. Between the measurements no external magnetic field was applied. The samples were stored at liquid nitrogen temperature (77 K), room temperature (293 K), and on a hotplate at 373 K (below the blocking temperature, $T_B = 500$ K^{18,19}) for 528 h and then all samples were stored at room temperature. The conditions for cooling and heating were used only for the storage of the samples. The ion bombardment and magnetic characterization were both performed at room temperature. Therefore, the samples have been removed for each magnetic characterization for about 1 min from their storage location.

III. RESULTS AND DISCUSSION

The modification of the exchange bias field as a function of time after ion bombardment in a bombardment field *parallel* to the original exchange bias direction normalized for the exchange bias field after field cooling is shown in Fig. 1 for samples stored at different temperatures. The same is shown in Fig. 2 for bombardment in a magnetic field *antiparallel* to the original exchange bias direction.

The ion bombardment in the parallel bombardment field geometry induced an enhancement of the exchange bias field to $H_{EB}(t = 1 \text{ h})/H_{EB,0} = 1.11$ one hour after the bombardment

^{a)}Electronic mail: schmidt@physik.uni-kassel.de.

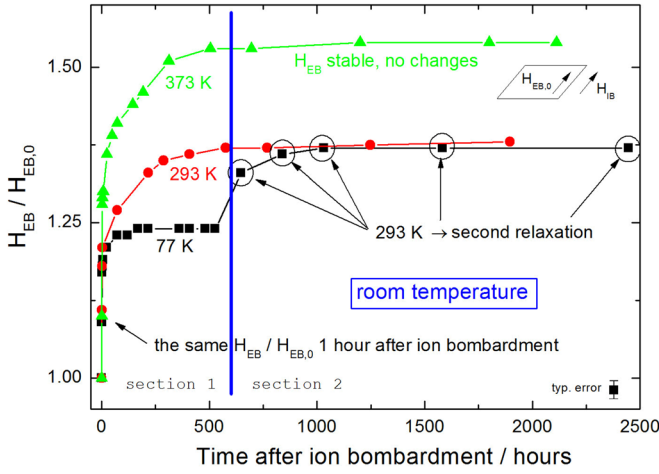


FIG. 1. (Color online) Temporal changes of H_{EB} (normalized to the initial value, $H_{EB,0}$, after field cooling) after 10 keV He ion bombardment with 1.0×10^{15} ions/cm² in parallel bombardment field geometry for different storage temperatures (see Sec. I). After 528 h, the cooling/heating was deactivated (see Sec. II) and the samples were stored at 293 K. Lines connecting the data points are guides to the eye.

which was almost independent of the storage temperature. Subsequently, an approximately logarithmic temporal change of the exchange bias field starts with different change rates at different temperatures. A magnified view of the first 100 h of the general effect can be found in Ref. 16. For longer times after bombardment, the logarithmic increase model fails since a saturation value seems to be approached. Saturation is reached faster at a lower storage temperature.

In the developed model¹⁶ the thermal aftereffect is described for certain time intervals by,

$$H_{EB}(t)/H_{EB,0} = h + \Delta h \cdot \ln(t), \quad (1)$$

where $H_{EB}(t)$ is the exchange bias field t hours after the ion bombardment normalized for the exchange bias field before ion bombardment, $H_{EB,0}$, and h and Δh are fit factors for the start and the logarithmic change rate of $H_{EB}(t)/H_{EB,0}$. In Eq. (2), Δh has been expressed by,

$$\Delta h = - \frac{N^{loc}(t=1h) \cdot \bar{\kappa}_{EB}}{\mu_0 M_{FM} d_{FM}} \cdot \frac{k_B T \ln(\nu_0)}{\bar{K}_{AF}(V_{min} - V_{max})}, \quad (2)$$

where $N^{loc}(t=1h)$ is the number of grains in the local free energy minima of the antiferromagnetic grains exchange coupled to the ferromagnet at $t=1h$, $\bar{\kappa}_{EB}$ is the exchange coupling constant, and \bar{K}_{AF} is the antiferromagnetic anisotropy

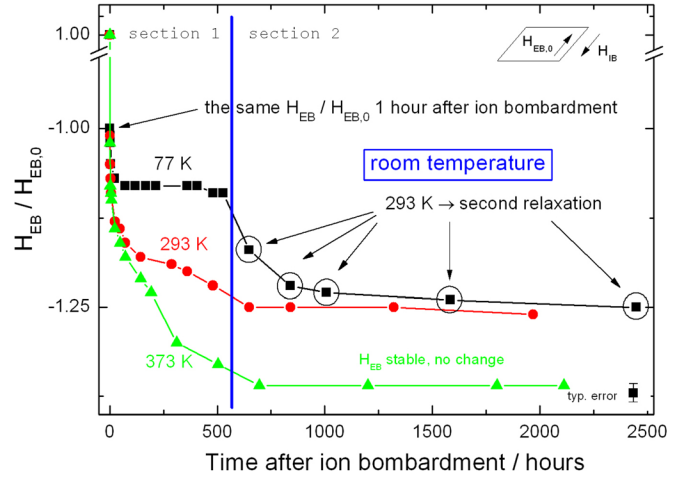


FIG. 2. (Color online) Same as Fig. 1, but ion bombardment in antiparallel bombardment field geometry with the same fluence.

ropy constant, both averaged over all grains, M_{FM} and d_{FM} are the saturation magnetization and thickness of the ferromagnet, $V_{min}(V_{max})$ is the minimal (maximal) volume of grains contributing to a stable exchange bias at the respective temperature, as outlined in Ref. 16. Here, μ_0 denotes the magnetic constant, $k_B T$ is the thermal energy, and ν_0 is the characteristic transition rate for a spin flip, which is usually assumed to be 10^{-9} s^{-1} .²⁰

The different graphs of Figs. 1 and 2 have been fitted by Eq. (1) and the determined parameters, h and Δh , are shown in Table I.

For the antiparallel bombardment field geometry, the basic behavior is very similar to bombardment in parallel bombardment field geometry, however, the unidirectional anisotropy is now rotated by 180 degrees.^{21,22}

As outlined in Ref. 16, Eqs. (1) and (2) are valid starting from a time when most of the coupling sites are already in their respective global free energy minimum. Therefore, all measurements have been started 1 h after ion bombardment, such that most of the coupling sites are already in their global free energy minimum. Additionally, a saturation effect for longer storage times is observed, which also cannot be described by Eqs. (1) and (2). From the present experiments, it is obvious that saturation occurs faster for smaller temperatures. Therefore, fits to Eq. (1) have been carried out for intermediate time intervals between 1 and 168 h for $T=77$ K, between 1 and 576 h for 293 K, and between 1 and 504 h for 373 K. The determined coefficients, Δh , as

TABLE I. Fit parameters determined by Eq. (1) from Figs. 1 and 2. The ΔH_{EB} is the absolute change of the exchange bias field from $t=1h$ to saturation after ion bombardment with a fluence of 1.0×10^{15} ions/cm².

Bombardment field geometry	T [K] (Sec. I)	ΔH_{EB} [kA/m] [$\pm 4\%$]	h [1] [$\pm 2\%$]	Δh [1/h] [$\pm 6\%$]	T [K] (Sec. II)	Δh [1/h] [$\pm 6\%$]
Parallel	77	1.12	1.13	0.0154	293	0.0349
	293	2.14	1.14	0.0365	293	stable
	373	3.95	1.16	0.0493	293	stable
Antiparallel	77	0.92	-1.00	-0.0132	293	-0.0294
	293	2.77	-1.02	-0.0331	293	stable
	373	4.35	-1.02	-0.0468	293	stable

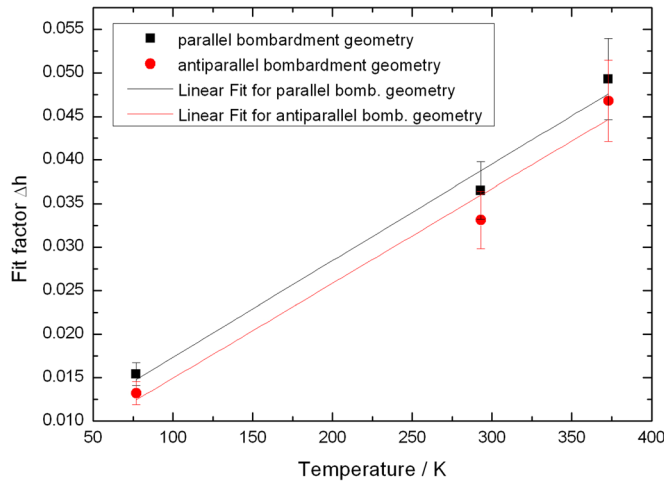


FIG. 3. (Color online) The Δh as a function of the storage temperature after bombardment in the parallel bombardment field geometry (black squares) and the antiparallel bombardment field geometry (red circles).

functions of temperature are plotted in Fig. 3. Within each bombardment field geometry Δh depends approximately linearly on T . Since Eqs. (1) and (2) also hold for polycrystalline exchange bias layers which have not been modified by ion bombardment, we have compared the model with the published experimental data³ of a different exchange bias layer system (NiO/NiFe). Figure 4 shows the data of Ref. 3, plotted logarithmically with fits by Eq. (1). As the inset of Fig. 4 shows, the determined coefficients, Δh , are also approximately linearly dependent on T , confirming the model of Ref. 16 and similar published models.⁶

The ion bombardment of the exchange bias layers gives a unique opportunity to test other consequences of the model. Experiments have been carried out with the same exchange bias layer system from the same batch. Therefore, for all samples, d_{FM} and M_{FM} of Eq. (2) are the same. Bombardment in the parallel and antiparallel field geometry has been carried out with the same fluence. Therefore, it is reasonable to assume that the average coupling and anisotropy constants $\bar{\kappa}_{\text{EB}}$ and $\bar{\kappa}_{\text{AF}}$ are the same for all samples and the grain size

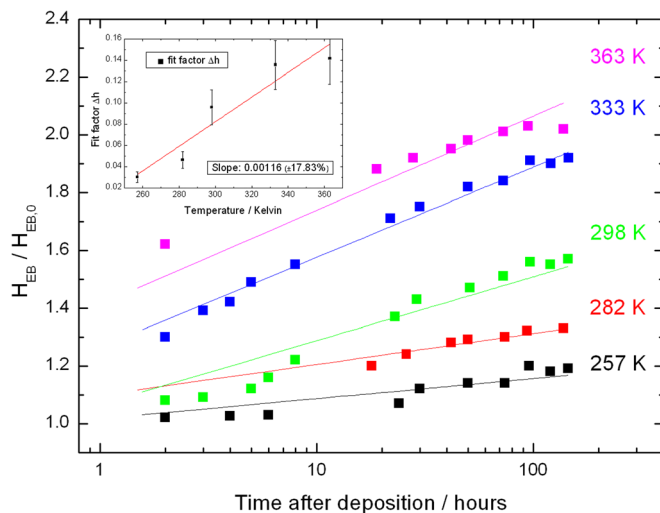


FIG. 4. (Color online) Published data of NiO/NiFe bilayers (see Fig. 2 of Ref. 3) with the logarithmic time scale. The inset shows the fit factor, Δh , as a function of the storage temperature.

distribution represented in Eq. (2) by $(V_{\text{min}} - V_{\text{max}})$. The only parameter which is changed by the ion bombardment in the parallel and antiparallel bombardment field geometry in a different way is $N^{\text{loc}}(t = 1 \text{ h})$. Bombardment in the parallel bombardment field geometry enhances the number of coupling sites with a global energy minimum toward the original exchange bias direction. Bombardment in the antiparallel field geometry, where in the free energy landscape the directions of local and global minima are exchanged, has to transfer the majority of coupling sites from the new local free energy minimum direction to the global one. Therefore, $N^{\text{loc}}(t = 1 \text{ h})$ for the antiparallel field geometry is smaller than $N^{\text{loc}}(t = 1 \text{ h})$ for the parallel bombardment field geometry, which in turn leads to a smaller Δh for the antiparallel field geometry at the same storage temperature. This is exactly what can be observed from Fig. 3.

Finally, the present experiments indicate that exchange bias field saturation is smaller at smaller temperatures. This is also explainable by the model used since at higher temperatures more coupling sites residing in the local energy minimum direction may overcome the energy barrier leading to higher exchange bias fields. Saturation for the present samples is reached faster at lower temperatures, also indicating the smaller number of coupling sites which energy barrier may be thermally overcome at a lower temperature.

IV. CONCLUSION

The present paper experimentally confirms the temporal change of the exchange bias field at different temperatures as proposed in recent models of the exchange bias field in polycrystalline layers. Using 10 keV He ion bombardment in different bombardment field geometries, it has been possible to confirm the proposed dependence of the logarithmic change rate with T and the influence of the initial number of coupling sites in our recently developed model.

¹S. S. P. Parkin, *Annual Review of Materials Science*, edited by B. W. Wessels (Annual Reviews Inc., Palo Alto, CA, 1995), Vol. 25, pp. 357–388.

²J. Fassbender, S. Poppe, T. Mewes, J. Juraszek, B. Hillebrands, K.-U. Barholz, R. Mattheis, D. Engel, M. Jung, H. Schmoranzer, and A. Ehresmann, *Appl. Phys. A* **77**, 51 (2003).

³A. Paetzold and K. Röhl, *J. Appl. Phys.* **91**, 7748 (2002).

⁴S. Soeya, M. Fuyama, S. Tadokoro, and T. Imagawa, *J. Appl. Phys.* **79**, 1604 (1996).

⁵J. Fujikata, K. Hayashi, H. Yamamoto, and M. Nakada, *J. Appl. Phys.* **83**, 7210 (1998).

⁶K. O'Grady, L. E. Fernandez-Outon, and G. Vallejo-Fernandez, *J. Magn. Magn. Mater.* **322**, 883 (2010).

⁷A. Ehresmann, D. Engel, T. Weis, A. Schindler, D. Junk, J. Schmalhorst, V. Höink, M. D. Sacher, and G. Reiss, *Phys. Status Solidi B* **243**, 29 (2006).

⁸A. Mougín, T. Mewes, R. Lopusnik, M. Jung, D. Engel, A. Ehresmann, H. Schmoranzer, J. Fassbender, and B. Hillebrands, *IEEE Trans. Magn.* **36**, 2647 (2000).

⁹J. Juraszek, J. Fassbender, S. Poppe, T. Mewes, B. Hillebrands, D. Engel, A. Kronenberger, A. Ehresmann, and H. Schmoranzer, *J. Appl. Phys.* **91**, 6896 (2002).

¹⁰V. Höink, M. Sacher, J. Schmalhorst, G. Reiss, D. Engel, D. Junk, and A. Ehresmann, *Appl. Phys. Lett.* **86**, 152102 (2005).

¹¹V. Höink, D. Meyners, J. Schmalhorst, G. Reiss, D. Junk, D. Engel, and A. Ehresmann, *Appl. Phys. Lett.* **91**, 162505 (2007).

¹²A. Mougín, S. Poppe, J. Fassbender, B. Hillebrands, G. Faini, U. Ebels, M. Jung, D. Engel, A. Ehresmann, and H. Schmoranzer, *J. Appl. Phys.* **89**, 6606 (2001).

- ¹³J. Fassbender, S. Poppe, T. Mewes, A. Mougin, B. Hillebrands, D. Engel, M. Jung, A. Ehresmann, H. Schmoranzer, G. Faini, K. J. Kirk, and J. N. Chapman, *Phys. Status Solidi A* **189**, 439 (2002).
- ¹⁴J. McCord, R. Schäfer, K. Theis-Bröhl, H. Zabel, J. Schmalhorst, V. Höink, H. Brückl, D. Engel, and A. Ehresmann, *J. Appl. Phys.* **97**, 10K102 (2005).
- ¹⁵K. Theis-Bröhl, M. Wolff, A. Westphalen, H. Zabel, J. McCord, V. Höink, J. Schmalhorst, G. Reiss, T. Weis, D. Engel, A. Ehresmann, U. Rücker, and B. P. Toperverg, *Phys. Rev. B* **73**, 174408 (2006).
- ¹⁶A. Ehresmann, C. Schmidt, T. Weis, and D. Engel, *J. Appl. Phys.* **109**, 023910 (2011).
- ¹⁷A. Ehresmann, D. Junk, D. Engel, A. Paetzold, and K. Roll, *J. Phys. D* **38**, 801 (2005).
- ¹⁸G. Anderson, Y. Huai, and L. Miloslawsky, *J. Appl. Phys.* **87**, 6989 (2000).
- ¹⁹M. Urbaniak, J. Schmalhorst, A. Thomas, H. Brückl, G. Reiss, T. Lucinski, and F. Stobiecki, *Phys. Status Solidi A* **199**, 284 (2003).
- ²⁰E. Fulcomer and S. H. Charap, *J. Appl. Phys.* **43**, 4190 (1972).
- ²¹A. Mougin, T. Mewes, M. Jung, D. Engel, A. Ehresmann, H. Schmoranzer, J. Fassbender, and B. Hillebrands, *Phys. Rev. B* **63**, 060409 (2001).
- ²²D. Engel, A. Kronenberger, M. Jung, H. Schmoranzer, A. Ehresmann, A. Paetzold, and K. Röhl, *J. Magn. Magn. Mater.* **263**, 275 (2003).